https://doi.org/10.5194/egusphere-2026-3774
Preprint. Discussion started: 14 July 2026

Post-SSW Quasi-Biweekly Oscillations Sustained by Wave-Mean Flow Feedback in the Southern Hemisphere

Yiran Pan[1], Jialin Zhang[1], Chengyun Yang[1,2], Tao Li[1,2], Xin Fang[1,2], Xinyue Wang[3], Xianghui Xue[1,2], Xiankang Dou[1,2]

[1]National Key Laboratory of Deep Space Exploration/School of Earth and Space Sciences, University of Science and Technology of China, Hefei, China
[2]CAS Center for Excellence in Comparative Planetology, University of Science and Technology of China, Hefei, China
[3]Department of Earth and Space Sciences, University of Colorado, Boulder, USA

Correspondence to: Chengyun Yang (cyyang@ustc.edu.cn) and Tao Li (litao@ustc.edu.cn)

Abstract. A quasi-biweekly oscillation developed in the Southern Hemisphere following the 2024 sudden stratospheric warming (SSW) events, rather than a monotonic recovery. Although recurrent tropospheric planetary-wave activity preceded the warming episodes, the much stronger stratospheric response suggests that lower-level forcing alone cannot explain the oscillation. We show that planetary-wave propagation, the polar vortex, and the stratospheric waveguide were linked through a coupled feedback: enhanced upward wave propagation before the warming peaks weakened and contracted the polar vortex, shifting the strongest waveguide structure poleward and reducing its overlap with the main 50°S–70°S wave-activity region. The subsequent weakening of upward propagation allowed the westerly flow and polar vortex to partially recover, restoring favorable propagation conditions and enabling the next cycle. These results suggest that Antarctic post-SSW variability can be sustained from late winter into early spring by internally modulated wave-mean flow interactions.

1 Introduction

Troposphere–stratosphere coupling regulates large-scale atmospheric variability across a wide range of timescales, particularly in the extratropics where planetary waves strongly influence the polar vortex, jet structure, and meridional circulation (Andrews et al., 1987; Baldwin et al., 2021). Planetary waves generated in the troposphere can propagate upward into the middle atmosphere, where they dissipate or break and deposit momentum and heat (Charney and Drazin, 1961; Matsuno, 1971). Through wave-mean flow interaction, this wave forcing can weaken, displace, or reshape the polar vortex. The resulting changes in winds and thermal structure modify atmospheric refractive properties, thereby regulating subsequent wave propagation, absorption, and reflection (Andrews et al., 1987; Matsuno, 1971; Hitchcock and Haynes, 2016).

When planetary-wave forcing becomes anomalously strong, wave-mean flow interactions can produce pronounced disturbances of the polar vortex. Sudden stratospheric warmings (SSWs) are among the most dramatic examples, characterized by rapid polar warming, weakening of the polar vortex, and circulation reorganization (Charlton and Polvani, 2007; Butler et

https://doi.org/10.5194/egusphere-2026-3774
Preprint. Discussion started: 14 July 2026

al., 2015). Their effects can extend downward into the troposphere, upward into the mesosphere and lower thermosphere, and persist for weeks to months (Baldwin and Dunkerton, 2001; White et al., 2019; Yang et al., 2022).

The onset and subsequent impacts of SSWs have been extensively studied. Previous work has identified several pathways to anomalous upward wave forcing, including enhanced tropospheric planetary-wave activity (Polvani and Waugh, 2004; Garfinkel et al., 2010), favorable vortex preconditioning (Albers and Birner, 2014), and internal stratospheric amplification (Matthewman and Esler, 2011; de la Cámara et al., 2017). Considerable progress has also been made in understanding the downward influence of SSWs (Baldwin and Dunkerton, 2001; White et al., 2020; Rupp et al., 2023). However, how the stratosphere reorganizes after an SSW remains less well understood, particularly when the polar vortex does not recover monotonically but instead supports renewed dynamical variability (Hitchcock et al., 2013). In this state, the evolving mean flow is not only a response to prior wave forcing but also a regulator of subsequent wave propagation. Clarifying this post-event evolution is important for understanding the persistence of SSW anomalies and their continuing role in vertical coupling.

The Southern Hemisphere provides a distinct setting for examining this post-event evolution. Compared with the Northern Hemisphere, its weaker climatological planetary-wave forcing and colder, stronger, and more symmetric winter polar vortex create a more stable background state (Baldwin et al., 2021; Jucker et al., 2021). The Antarctic stratosphere therefore exhibits reduced variability and far fewer extreme warmings. Since the satellite era began, only one major Antarctic SSW has been observed, in 2002, together with the minor warming event of 2019 (Charlton et al., 2005; Shen et al., 2020; Lim et al., 2021). The rarity of these events has limited observational constraints on how the Antarctic stratosphere evolves and adjusts following an SSW. In austral winter 2024, however, the Antarctic stratosphere experienced two consecutive minor SSWs in July and August, followed by unusual recurrent warming episodes rather than a gradual return toward climatology (Zi et al., 2025; Lim et al., 2026). The dynamical origin of this recurrent post-SSW variability remains unclear, particularly under the weak climatological wave forcing of the Southern Hemisphere.

To address this issue, we analyze the Antarctic atmosphere during the 2024 austral winter using reanalysis diagnostics. We focus on the processes controlling the repeated warming episodes following the initial SSWs, with particular attention to how wave forcing, the polar vortex, and the stratospheric waveguide evolved together. This case provides a rare opportunity to investigate how post-SSW variability develops and persists in the Southern Hemisphere, and to assess the possible role of wave-mean flow interactions in shaping this variability.

2 Results

Figure 1a and b show the temporal evolution of polar-cap temperature anomalies and zonal wind anomalies during July–September (JAS) 2024. Two SSW events are evident in July and early August, both characterized by strong polar warming and pronounced deceleration of the polar night jet (Zi et al., 2025). Rather than relaxing monotonically toward climatology after the initial SSWs, the stratosphere underwent three additional warming episodes around 23 August, 3 September, and 13 September, each accompanied by renewed deceleration of the zonal wind (Lim et al., 2026). Together,

https://doi.org/10.5194/egusphere-2026-3774
Preprint. Discussion started: 14 July 2026

these events define a recurrent warming–recovery pattern with a quasi-biweekly timescale in both temperature and zonal wind (Fig. 1a, b), raising the question of what sustained the repeated stratospheric warming episodes.

Given the central role of planetary-wave forcing in driving stratospheric variability (Matsuno, 1971; Andrews et al., 1987), we also examine the temporal relationship between stratospheric variability and planetary-wave activity using the time series of 50 hPa eddy heat flux anomalies (Fig. 1d). In the Southern Hemisphere, negative eddy heat flux anomalies over 45°S–75°S indicate enhanced upward planetary-wave activity entering the lower stratosphere. Each warming episode is preceded by negative 50 hPa eddy heat flux anomalies, indicating enhanced upward wave propagation before the warming peak. The associated westward momentum deposition would decelerate the westerly polar night jet and weaken the stratospheric polar vortex, consistent with the subsequent zonal wind anomalies (Fig. 1c). Following each warming peak, the eddy heat flux anomalies turn positive, indicating suppressed upward wave activity after the vortex has weakened. This repeating sequence of enhanced wave forcing before warming and suppressed wave activity afterward suggests that planetary-wave forcing is closely linked to the quasi-biweekly oscillation, while the changing propagation conditions require further diagnosis.

https://doi.org/10.5194/egusphere-2026-3774
Preprint. Discussion started: 14 July 2026

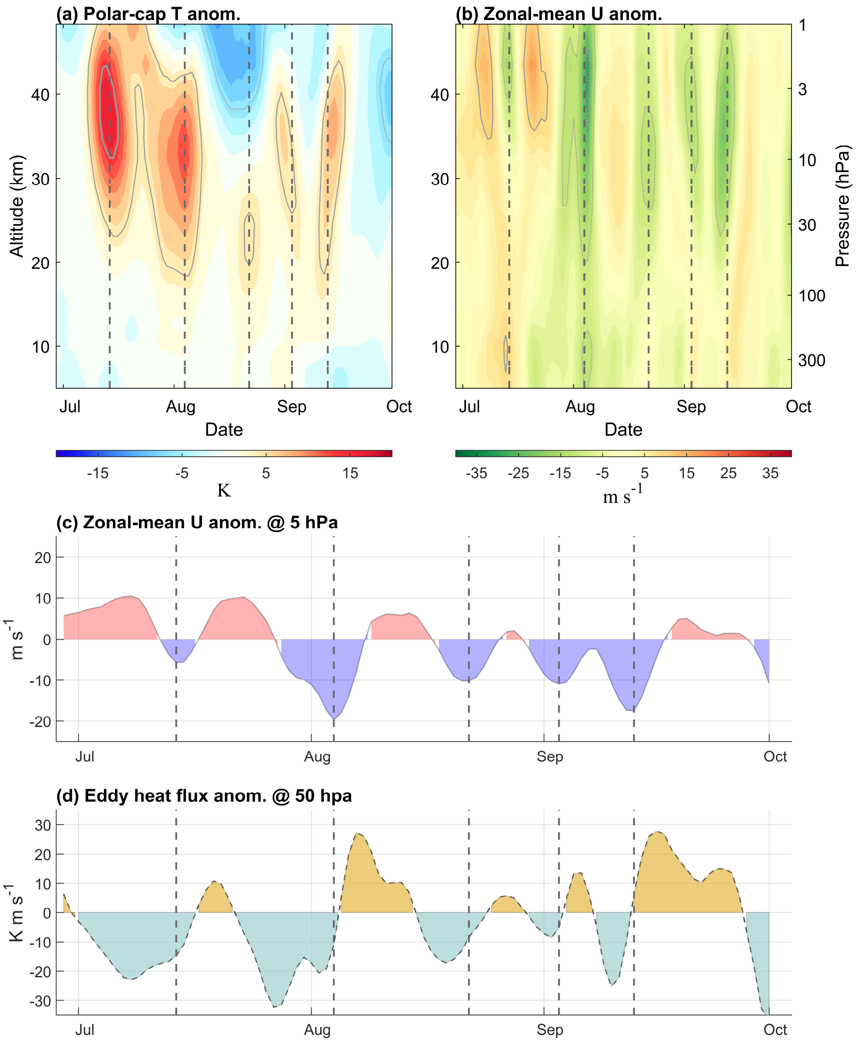

Figure 1: Time-height cross-sections of daily (a) zonal-mean polar cap temperature anomalies (averaged over 60°S–90°S) and (b) zonal-mean zonal wind anomalies (averaged over 55°S–65°S) during July–September (JAS) 2024. Time series of daily (c) zonal-mean zonal wind anomalies (averaged over 55°S–65°S) at 5 hPa, and (d) eddy heat flux anomalies (averaged over 45°S–75°S) at 50 hPa. Gray vertical dashed lines indicate the dates corresponding to the peaks of the stratospheric warming events.

To further assess how tropospheric wave activity was linked to the stratospheric response, Figure 2 compares the amplitudes of zonal wavenumbers 1 and 2 at 500 hPa and 10 hPa. During the two initial SSW events, enhanced wave activity is evident at both 500 hPa and 10 hPa, consistent with previous reports of anomalous planetary-wave forcing associated with the 2024 Antarctic warmings (Zi et al., 2025). Notably, the amplification is much more pronounced at 10 hPa than at 500 hPa. The 10 hPa wave-1 amplitude during the first event peaks around 14–15 July and exceeds 2.5 times its climatological mean (Fig. 2c), while the 10 hPa wave-2 amplitude during the second event reaches approximately four times its climatological

https://doi.org/10.5194/egusphere-2026-3774
Preprint. Discussion started: 14 July 2026

mean (Fig. 2d). This vertical contrast suggests that the evolving stratospheric background state likely played an important role in modulating the upward propagation and amplification of planetary waves.

Turning to the three subsequent warming episodes, wave-1 activity at 500 hPa shows recurrent enhancements before the events, indicating recurrent variations in tropospheric planetary-wave activity (Fig. 2a). However, these lower-level wave-1 anomalies remain close to the climatological range and are much weaker than the corresponding 10 hPa response, where wave-1 amplitudes approach or exceed the climatological maxima. This vertical contrast indicates that the quasi-biweekly stratospheric variability cannot be explained by tropospheric wave forcing alone. The wave-2 diagnostics further support this interpretation: although 500 hPa wave-2 activity is enhanced during 12–20 August, the corresponding stratospheric response is not comparably strong. Thus, enhanced tropospheric wave activity does not necessarily lead to an amplified stratospheric wave response. These results point to an important role of the evolving stratospheric background state in regulating whether lower-level planetary waves can propagate upward and amplify.

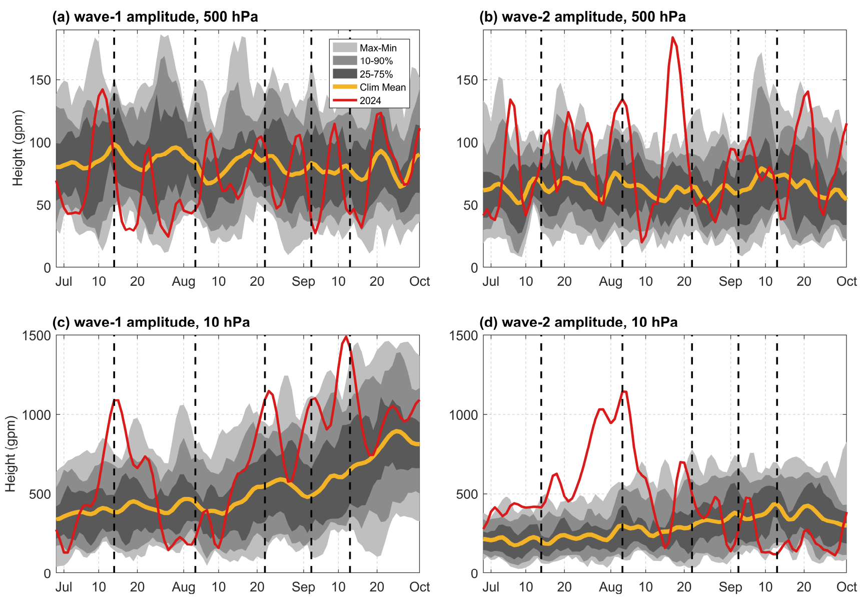

Figure 2: Time series of daily geopotential height amplitudes for (a) zonal wavenumber 1 at 500 hPa, (b) zonal wavenumber 2 at 500 hPa, (c) zonal wavenumber 1 at 10 hPa, and (d) zonal wavenumber 2 at 10 hPa during JAS 2024. All amplitudes are averaged over the 45°S–75°S latitude band. Yellow lines represent the daily climatology computed from 2003 to 2023. Gray shading denotes the daily 25th–75th percentile range (dark), 10th–90th percentile range (medium), and minimum–maximum range (light) for austral winters during 2003–2023. Vertical dashed lines are as in Fig. 1.

We therefore examine the background structure controlling planetary-wave propagation during July–September (JAS) 2024. The austral winter of 2024 exhibited a highly anomalous stratospheric background state. As shown in Fig. 3a, the JAS-mean zonal-mean zonal wind anomalies are characterized by a distinct meridional dipole pattern, associated with a marked

https://doi.org/10.5194/egusphere-2026-3774
Preprint. Discussion started: 14 July 2026

deceleration north of 60°S and a concurrent acceleration to the south. This dipole structure indicates a pronounced poleward contraction of the Antarctic polar vortex (Lim et al., 2026). This structural change in the vortex is accompanied by a reshaped stratospheric waveguide, as diagnosed by the JAS-mean anomalies of the refractive index squared, n^2, for stationary zonal wavenumber 1 (Fig. 3b). Positive n^2 denotes regions where planetary waves can propagate, while the zero contour marks the approximate boundary of the waveguide (Matsuno, 1970; Li et al., 2007). Compared with the climatological mean, n^2 in 2024 is markedly enhanced in the stratosphere between 60°S and 75°S, and the zero contour shifts poleward. This indicates that the post-SSW background state produced a stronger stratospheric waveguide that extended farther poleward, providing more favorable propagation conditions for planetary waves in this region.

Although the JAS-mean field indicates a generally favorable waveguide in 2024, this mean-state view does not explain why the warming events recurred with a quasi-biweekly timescale. We therefore examine the time-dependent evolution of wave activity and waveguide strength. Figure 3c presents the latitude-time cross-section of eddy heat flux at 100 hPa. The episodic pulses of upward wave activity are mainly confined to 50°S–70°S, consistent with the high-latitude waveguide identified in Fig. 3b. After the 14 July warming, the eddy heat flux turns positive only briefly and then remains predominantly negative, indicating that upward planetary-wave activity was largely maintained during the early stage. In contrast, after the early-August and later warmings, eddy heat flux reverses to positive values over broad latitude ranges, indicating repeated suppression of upward wave activity. Although the timing and meridional extent of the suppression differ among events, the pattern is consistent: upward wave activity is enhanced before the warming peaks and suppressed afterward.

Accordingly, Figure 3d shows the temporal evolution of the area-averaged refractive index squared (n^2) over the core propagation region (50°S–70°S, 100–1 hPa). Consistent with the JAS-mean enhancement shown in Fig. 3b, n^2 is generally higher than its climatological mean during JAS 2024, indicating an overall more favorable background waveguide. However, this enhanced waveguide is not steady. Following each warming event, n^2 weakens to different degrees: the reduction is relatively moderate after the first two warmings, brings n^2 back close to climatology after the late-August event, and drives it below the climatological mean after the early- and mid-September events. In each case, n^2 subsequently increases again, reaching values clearly above climatology before the next warming episode.

Because positive n^2 values denote conditions favorable for stationary planetary-wave propagation, these repeated decreases and recoveries indicate an event-scale weakening and restoration of the stratospheric waveguide. This event-scale modulation coincides with the repeated enhancement and suppression of eddy heat flux shown in Fig. 3c, suggesting that recurrent wave activity entering the stratosphere was accompanied by corresponding changes in waveguide strength.

https://doi.org/10.5194/egusphere-2026-3774
Preprint. Discussion started: 14 July 2026

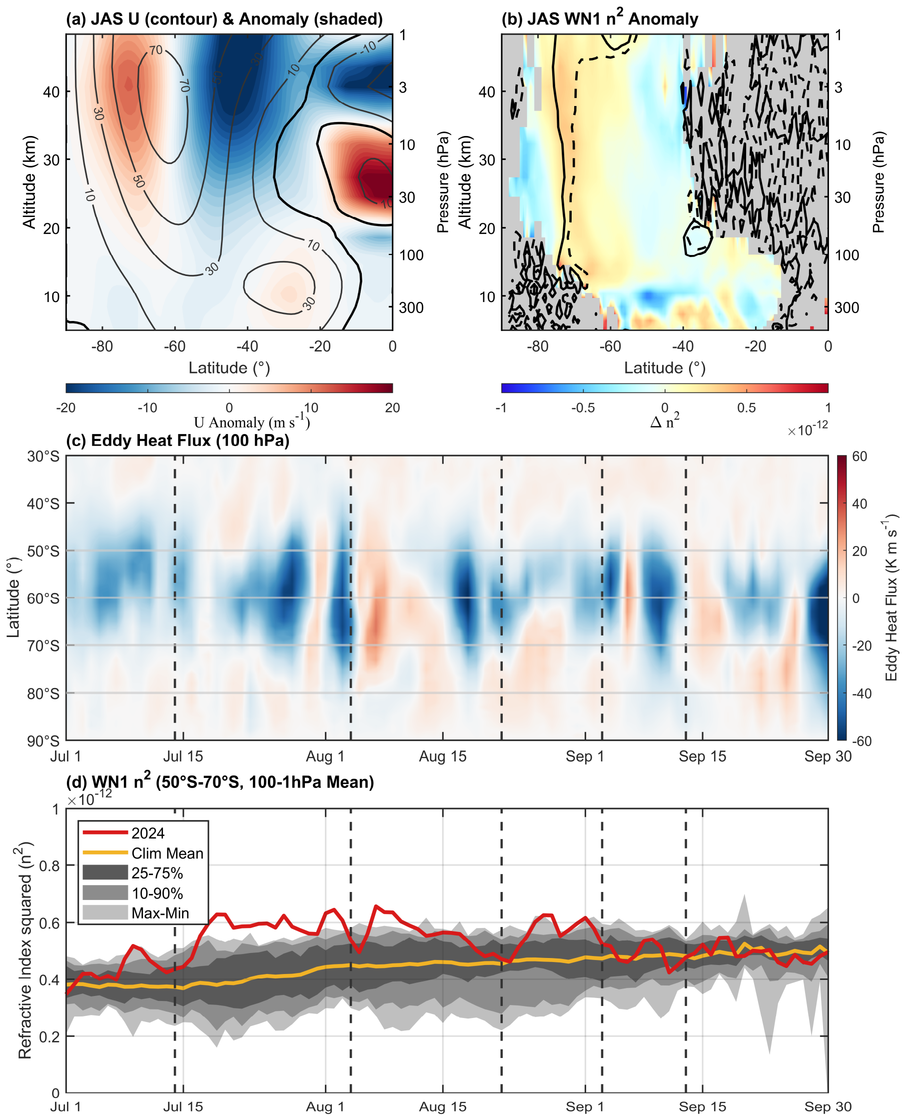

Figure 3: (a) 2024 JAS-mean latitude-height distribution of zonal-mean zonal wind (contour) and its anomalies (shaded). (b) JAS-mean anomalies of refractive index squared, n^2, for stationary zonal wavenumber 1. Gray shading indicates masked regions where n^2 anomalies are unavailable or exceed the colorbar range of ±1.0 × 10^{-12}. Black solid and dashed contours represent the zero contours of n^2 for 2024 and the climatological mean, respectively. (c) Time-latitude distribution of eddy heat flux ($\overline{v'T'}$) at 100 hPa. (d) Time series of the area-averaged n^2 over the core propagation region (50°S–70°S, 100–1 hPa). Vertical dashed lines in (c) and (d) are as in Fig. 1.

In sum, Figure 3 shows that the stratospheric waveguide varied with the repeated warming–recovery cycle, but the refractive index squared alone does not identify which component of the background state controlled this modulation. To diagnose the dynamical origin of the waveguide variability, we examine the meridional gradient of zonal-mean QGPV, $\bar{q}_\phi$. This quantity appears in the leading dynamical term of the refractive index for stationary planetary waves and is strongly

https://doi.org/10.5194/egusphere-2026-3774
Preprint. Discussion started: 14 July 2026

influenced by the horizontal and vertical shear of the zonal-mean wind. It therefore provides a link between changes in vortex structure, waveguide variability, and the conditions for planetary-wave propagation.

Figure 4a shows that the $\overline{q}_\phi$ anomalies evolve coherently with the warming–recovery cycle and the meridional displacement of the polar vortex. Before the first SSW, positive $\overline{q}_\phi$ anomalies are mainly located around 50°S–60°S, while weaker or negative anomalies appear at higher latitudes. As the first SSW develops, the positive $\overline{q}_\phi$ anomalies rapidly intensify and shift poleward, with the anomaly center moving toward 70°S–80°S. This evolution is broadly consistent with the zonal-wind anomalies in Fig. 4b, indicating a rapid contraction of the Antarctic polar vortex and a redistribution of $\overline{q}_\phi$ anomalies toward higher latitudes. As a result, the strongest $\overline{q}_\phi$ anomalies shift toward 70°S–80°S, contributing to a poleward displacement of the waveguide relative to the main 50°S–70°S wave-activity band.

The latitude-dependent $\overline{q}_\phi$ anomalies further clarify why the waveguide variability most strongly affects the main propagation region. In the 50°S–70°S band, where the lower-stratospheric eddy heat flux is strongest, $\overline{q}_\phi$ decreases during the warming peaks and recovers afterward, closely matching the event-scale variations in refractive index squared shown in Fig. 3d. By contrast, $\overline{q}_\phi$ enhancements during the warming events are concentrated farther poleward, near 70°S–80°S. Because lower-stratospheric eddy heat flux is weaker there, these polar-side $\overline{q}_\phi$ enhancements are less directly connected to the main upward planetary-wave activity. This meridional displacement reduces the overlap between the strongest waveguide structure and the primary wave-activity region, providing a mechanism that suppresses subsequent upward propagation.

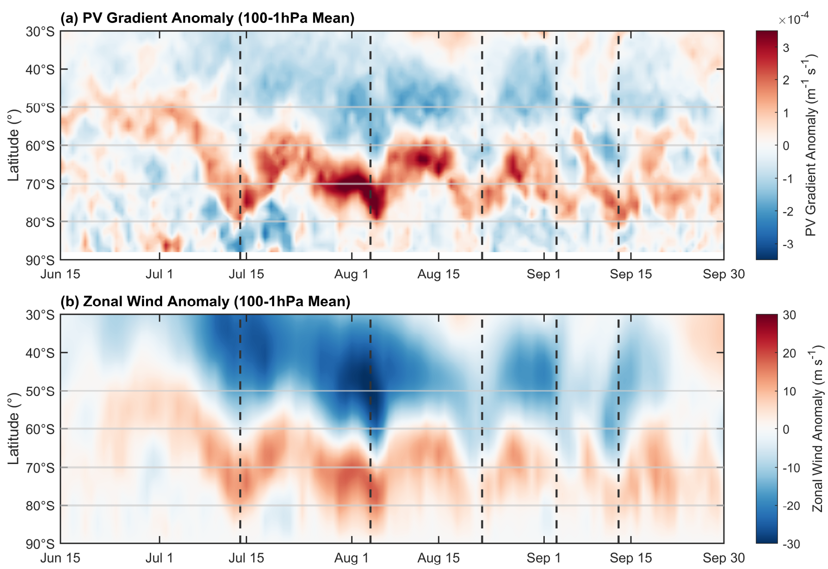

Figure 4: Time-latitude distribution of the vertically averaged (100–1 hPa) anomalies for (a) meridional quasi-geostrophic potential vorticity gradient ($\overline{q}_\phi$) and (b) zonal-mean zonal wind. Vertical dashed lines are as in Fig. 1.

https://doi.org/10.5194/egusphere-2026-3774
Preprint. Discussion started: 14 July 2026

Together, these results suggest that the quasi-biweekly variability reflects a repeated feedback among wave forcing, mean-flow adjustment, and waveguide displacement. Before each warming episode, favorable waveguide conditions in the 50°S–70°S band support upward planetary-wave propagation and associated easterly forcing on the polar night jet. The resulting weakening and contraction of the vortex displaces the strongest $\bar{q}_{\phi}$ and waveguide structure poleward, reducing its overlap with the main wave-activity region and suppressing subsequent upward propagation. As wave forcing weakens, the westerly flow and vortex edge partially recover, restoring a more favorable alignment between the waveguide and the wave-activity region. Repetition of this adjustment provides a dynamical pathway for the observed quasi-biweekly oscillation.

3 Conclusions

This study examines the unusual post-SSW evolution of the Southern Hemisphere stratosphere during austral winter 2024. Following two minor SSW events in July and early August, the stratosphere did not simply relax toward climatology. Instead, three additional warming episodes occurred from late August to mid-September, forming a coherent quasi-biweekly oscillation in temperature and zonal wind. This behavior indicates that the post-SSW atmosphere remained dynamically active for nearly two months, rather than undergoing a passive recovery after the initial warmings.

The oscillation was closely linked to repeated changes in planetary-wave activity and the evolving stratospheric waveguide. Recurrent lower-level planetary-wave forcing preceded the warming episodes, but the much stronger stratospheric response indicates that tropospheric forcing alone cannot explain the variability. During 2024, the post-SSW background state produced an enhanced high-latitude waveguide in the 50°S–70°S core propagation region. However, this waveguide was not steady: the refractive index squared decreased during warming peaks and recovered afterward, in step with the repeated enhancement and suppression of eddy heat flux. Further analysis of the meridional gradient of zonal-mean QGPV suggests that these waveguide changes were tied to meridional displacements of the polar vortex edge, which altered the alignment between the waveguide and the main wave-activity region.

These results suggest that the 2024 Southern Hemisphere post-SSW variability was organized by coupled feedback among wave forcing, mean flow, and the waveguide, rather than by a set of isolated warming events. The event therefore provides a rare example of how an Antarctic SSW can trigger a prolonged dynamical adjustment extending from late winter into early spring. This finding highlights the importance of the evolving stratospheric background state in controlling post-SSW variability, especially in the Southern Hemisphere where strong polar vortices and weak climatological wave forcing make such events rare. More broadly, the results imply that the impacts of SSWs may persist beyond the initial warming through internally modulated wave-mean flow interactions, with consequences for understanding extended vertical coupling in the winter atmosphere.

https://doi.org/10.5194/egusphere-2026-3774
Preprint. Discussion started: 14 July 2026

Appendix A: Data and Methods

To analyze the atmospheric variability following the 2024 Southern Hemisphere SSWs, we use meteorological fields from the fifth-generation atmospheric reanalysis produced by the European Centre for Medium-Range Weather Forecasts (ERA5; Hersbach et al., 2020). In this study, we use hourly temperature, zonal wind, meridional wind, vertical pressure velocity, and geopotential height fields on pressure levels for the period 2003–2024. The data are provided at a horizontal resolution of 0.25° × 0.25° and on 37 pressure levels extending from 1000 to 1 hPa. To assess whether the repeated warming events were associated with recurrent planetary-wave forcing, planetary-wave activity is diagnosed from the geopotential height field. The zonal wavenumber-1 and wavenumber-2 components are extracted using a spatial Fourier transform. For consistency with the dynamical diagnostics, all variables are averaged to daily means. Daily anomalies for 2024 are calculated as deviations from the corresponding daily climatology over 2003–2023.

The meridional eddy heat flux ($\overline{v'T'}$) is used as a diagnostic of upward planetary-wave activity entering the stratosphere (Newman and Nash, 2000), where v is the meridional wind, T is temperature, overbars denote zonal means, and primes indicate deviations from the zonal mean. To diagnose the background state of the atmosphere following the SSW event, the meridional gradient of the zonal-mean quasi-geostrophic potential vorticity (QGPV), denoted as $\bar{q}_\phi$, is calculated as follows (Meyer and Forbes, 1997):

$$\bar{q}_\phi = 2\Omega \cos\phi - \left(\frac{(\bar{u}\cos\phi)_\phi}{a\cos\phi}\right)_\phi - \frac{a}{\rho}\left(\frac{f^2}{N^2}\rho\bar{u}_z\right)_z \tag{1}$$

where ϕ is latitude, z is log-pressure altitude, u is the zonal wind, ρ is the air density, Ω is the angular velocity of the Earth's rotation, a is the Earth's radius, f is the Coriolis parameter, and N represents the Brunt-Väisälä frequency. Subscripts ϕ and z denote partial derivatives with respect to latitude and log-pressure altitude, respectively. Large positive $\bar{q}_\phi$ values indicate sharp PV gradients near the polar vortex edge, thereby providing a diagnostic of changes in vortex-edge structure.

To diagnose the propagation conditions for planetary waves entering the stratosphere, the refractive index squared (n^2) for stationary Rossby waves is calculated (Matsuno, 1970; Li et al., 2007). For a specific zonal wavenumber s, n^2 is defined as:

$$n^2 = \frac{\bar{q}_\phi}{a\bar{u}} - \frac{s^2}{a^2\cos^2\phi} - \frac{f^2}{4N^2H^2} \tag{2}$$

where H is the scale height. $\bar{q}_\phi$ forms the leading dynamical term in the refractive index for stationary Rossby waves, linking the vortex structure to the background conditions for planetary-wave propagation. As discussed by Matsuno (1970), planetary waves propagate in regions where $n^2 > 0$ and are refracted away from regions where $n^2 < 0$. Moreover, larger values of n^2 correspond to conditions more conducive to wave propagation, except at the critical level, where $\bar{u}$ approaches zero and n^2 becomes infinite. Therefore, the spatial distribution and magnitude of n^2 are used as diagnostics of the stratospheric waveguide in this study.

Data availability

ERA5 hourly data on pressure levels are available from the Copernicus Climate Change Service Climate Data Store at https://doi.org/10.24381/cds.bd0915c6 (Hersbach et al., 2023). The processed data used to generate the figures in this study are available at https://doi.org/10.5281/zenodo.20838731 (Pan, 2026).

Author contributions

YP and JZ contributed equally to this work. CY and TL conceived the study and supervised the project. YP and JZ performed the analysis and prepared the figures. XF, XW, XX, and XD contributed to the interpretation of the results. YP wrote the initial manuscript draft, and all authors reviewed and edited the manuscript.

Competing interests

The authors declare that they have no competing interests.

Acknowledgements

The authors acknowledge the European Centre for Medium-Range Weather Forecasts and the Copernicus Climate Change Service for providing ERA5 data.

Financial support

This work was supported by the National Natural Science Foundation of China (grant nos. 42130203 and 42275133), and the National Key R&D Program of China (grant no. 2022YFF0503703).

References

Albers, J. R., and Birner, T.: Vortex Preconditioning due to Planetary and Gravity Waves prior to Sudden Stratospheric Warmings. Journal of the Atmospheric Sciences, 71(11), 4028–4054, https://doi.org/10.1175/JAS-D-14-0026.1, 2014.

Andrews, D. G., Holton, J. R., and Leovy, C. B.: Middle atmosphere dynamics. Academic Press, 1987.

Baldwin, M. P., Ayarzagüena, B., Birner, T., Butchart, N., Butler, A. H., Charlton-Perez, A. J., et al.: Sudden Stratospheric Warmings. Reviews of Geophysics, 59(1), e2020RG000708, https://doi.org/10.1029/2020RG000708, 2021.

Baldwin, M. P., and Dunkerton, T. J.: Stratospheric harbingers of anomalous weather regimes. Science, 294, 581–584, https://doi.org/10.1126/science.1063315, 2001.

https://doi.org/10.5194/egusphere-2026-3774
Preprint. Discussion started: 14 July 2026

Butler, A. H., Seidel, D. J., Hardiman, S. C., Butchart, N., Birner, T., and Match, A.: Defining Sudden Stratospheric Warmings. Bulletin of the American Meteorological Society, 96(11), 1913–1928, https://doi.org/10.1175/BAMS-D-13-00173.1, 2015.

Cámara, A. D. L., Albers, J. R., Birner, T., Garcia, R. R., Hitchcock, P., Kinnison, D. E., and Smith, A. K.: Sensitivity of Sudden Stratospheric Warmings to Previous Stratospheric Conditions, Journal of the Atmospheric Sciences, 74, 2857–2877, https://doi.org/10.1175/JAS-D-17-0136.1, 2017.

Charlton, A. J., O'Neill, A., Lahoz, W. A., and Berrisford, P.: The splitting of the stratospheric polar vortex in the Southern Hemisphere, September 2002: Dynamical evolution. Journal of the Atmospheric Sciences, 62(3), 590–602, https://doi.org/10.1175/JAS-3318.1, 2005.

Charlton, A. J., and Polvani, L. M.: A New Look at Stratospheric Sudden Warmings. Part I: Climatology and Modeling Benchmarks. Journal of Climate, 20(3), 449–469, https://doi.org/10.1175/JCLI3996.1, 2007.

Charney, J. G., and Drazin, P. G.: Propagation of planetary-scale disturbances from the lower into the upper atmosphere. Journal of Geophysical Research, 66, 83–109, https://doi.org/10.1029/JZ066i001p00083, 1961.

Garfinkel, C. I., Hartmann, D. L., and Sassi, F.: Tropospheric Precursors of Anomalous Northern Hemisphere Stratospheric Polar Vortices. Journal of Climate, 23(12), 3282–3299, https://doi.org/10.1175/2010JCLI3010.1, 2010.

Hersbach, H., Bell, B., Berrisford, P., Hirahara, S., Horányi, A., Muñoz-Sabater, J., et al.: The ERA5 global reanalysis. Quarterly Journal of the Royal Meteorological Society, 146(730), 1999–2049, https://doi.org/10.1002/qj.3803, 2020.

Hersbach, H., Bell, B., Berrisford, P., Biavati, G., Horányi, A., Muñoz Sabater, J., et al.: ERA5 hourly data on pressure levels from 1940 to present [Dataset]. Copernicus Climate Change Service (C3S) Climate Data Store (CDS), https://doi.org/10.24381/cds.bd0915c6, 2023.

Hitchcock, P., Shepherd, T. G., and Manney, G. L.: Statistical Characterization of Arctic Polar-Night Jet Oscillation Events. Journal of Climate, 26(6), 2096–2116, https://doi.org/10.1175/JCLI-D-12-00202.1, 2013.

Hitchcock, P., and Haynes, P. H.: Stratospheric control of planetary waves. Geophysical Research Letters, 43, 11884–11892, https://doi.org/10.1002/2016GL071372, 2016.

Jucker, M., Reichler, T., and Waugh, D. W.: How frequent are Antarctic sudden stratospheric warmings in present and future climate? Geophysical Research Letters, 48, e2021GL093215, https://doi.org/10.1029/2021GL093215, 2021.

Li, Q., Graf, H.-F., and Giorgetta, M. A.: Stationary planetary wave propagation in Northern Hemisphere winter – climatological analysis of the refractive index. Atmospheric Chemistry and Physics, 7(1), 183–200, https://doi.org/10.5194/acp-7-183-2007, 2007.

Lim, E.-P., Hendon, H. H., Butler, A. H., Thompson, D. W. J., Lawrence, Z. D., Scaife, A. A., et al.: The 2019 Southern Hemisphere Stratospheric Polar Vortex Weakening and Its Impacts. Bulletin of the American Meteorological Society, 102(6), E1150–E1171, https://doi.org/10.1175/BAMS-D-20-0112.1, 2021.

Lim, E.-P., Thompson, D. W. J., Butler, A. H., Wheeler, M. C., Nakamura, H., Jucker, M., et al.: Characteristics of Antarctic Stratospheric Variability During Winter: A Case Study of the 2024 Sudden Stratospheric Warming and Its Surface Impacts. Journal of Geophysical Research: Atmospheres, 131(1), e2025JD045089, https://doi.org/10.1029/2025JD045089, 2026.

https://doi.org/10.5194/egusphere-2026-3774
Preprint. Discussion started: 14 July 2026

Matsuno, T.: Vertical Propagation of Stationary Planetary Waves in the Winter Northern Hemisphere. Journal of the Atmospheric Sciences, 27(6), 871–883, https://doi.org/10.1175/1520-0469(1970)027%3C0871:VPOSPW%3E2.0.CO;2, 1970.

Matsuno, T.: A Dynamical Model of the Stratospheric Sudden Warming. Journal of the Atmospheric Sciences, 28(8), 1479–1494, https://doi.org/10.1175/1520-0469(1971)028%3C1479:ADMOTS%3E2.0.CO;2, 1971.

Matthewman, N. J., and Esler, J. G.: Stratospheric Sudden Warmings as Self-Tuning Resonances. Part I: Vortex Splitting Events. Journal of the Atmospheric Sciences, 68(11), 2481–2504, https://doi.org/10.1175/JAS-D-11-07.1, 2011.

Meyer, C. K., and Forbes, J. M.: A 6.5-day westward propagating planetary wave: Origin and characteristics. Journal of Geophysical Research: Atmospheres, 102(D22), 26173–26178, https://doi.org/10.1029/97JD01464, 1997.

Newman, P. A., and Nash, E. R.: Quantifying the wave driving of the stratosphere. Journal of Geophysical Research: Atmospheres, 105(D10), 12485–12497, https://doi.org/10.1029/1999JD901191, 2000.

Pan, Y.: Post-SSW quasi-biweekly oscillations sustained by wave-mean flow feedback in the Southern Hemisphere, Zenodo [data set], https://doi.org/10.5281/zenodo.20838731, 2026.

Polvani, L. M., and Waugh, D. W.: Upward Wave Activity Flux as a Precursor to Extreme Stratospheric Events and Subsequent Anomalous Surface Weather Regimes. Journal of Climate, 17(18), 3548–3554, https://doi.org/10.1175/1520-0442(2004)017%3C3548:UWAFAA%3E2.0.CO;2, 2004.

Rupp, P., Spaeth, J., Garny, H., and Birner, T.: Enhanced polar vortex predictability following sudden stratospheric warming events. Geophysical Research Letters, 50, e2023GL104057, https://doi.org/10.1029/2023GL104057, 2023.

Shen, X., Wang, L., and Osprey, S.: Tropospheric Forcing of the 2019 Antarctic Sudden Stratospheric Warming. Geophysical Research Letters, 47(20), e2020GL089343, https://doi.org/10.1029/2020GL089343, 2020.

White, I., Garfinkel, C. I., Gerber, E. P., Jucker, M., Aquila, V., and Oman, L. D.: The Downward Influence of Sudden Stratospheric Warmings: Association with Tropospheric Precursors. Journal of Climate, 32(1), 85–108, https://doi.org/10.1175/JCLI-D-18-0053.1, 2019.

White, I. P., Garfinkel, C. I., Gerber, E. P., Jucker, M., Hitchcock, P., and Rao, J.: The Generic Nature of the Tropospheric Response to Sudden Stratospheric Warmings. Journal of Climate, 33(13), 5589–5610, https://doi.org/10.1175/JCLI-D-19-0697.1, 2020.

Yang, C., Li, T., Lai, D., Wang, X., Xue, X., and Dou, X.: The Delayed Response of the Troposphere-Stratosphere-Mesosphere Coupling to the 2019 Southern SSW. Geophysical Research Letters, 49(23), e2022GL101759, https://doi.org/10.1029/2022GL101759, 2022.

Zi, Y., Long, Z., Sheng, J., Lu, G., Perrie, W., and Xiao, Z.: The Sudden Stratospheric Warming Events in the Antarctic in 2024. Geophysical Research Letters, 52(7), e2025GL115257, https://doi.org/10.1029/2025GL115257, 2025.